

Investigation of AlMe₃, BEt₃, and ZnEt₂ as Co-Reagents for Low-Temperature Copper Metal ALD/Pulsed-CVD

Balamurugan Vidjayacoumar,[†] David J. H. Emslie,^{*,†} Scott B. Clendenning,^{*,‡}
James M. Blackwell,[‡] James F. Britten,[†] and Arnold Rheingold[§]

[†]Department of Chemistry, McMaster University, 1280 Main Street West, Hamilton, Ontario L8S 4M1, Canada, [‡]Intel Corporation, RA3-252, 2501 Northwest 229th Avenue, Hillsboro, Oregon 97124, and [§]Department of Chemistry and Biochemistry, University of California—San Diego, 9500 Gilman Drive, MC 0332, La Jolla, California, 92093-0332

Received May 22, 2010. Revised Manuscript Received July 13, 2010

The reactions of AlMe₃, BEt₃, and ZnEt₂ with toluene solutions of the copper(II) complexes [CuL₂] {L = acetylacetonate (acac; **1**), hexafluoroacetylacetonate (hfac; **2**), *N*-isopropyl- β -ketiminate (acnac; **3**), *N,N*-dimethyl- β -diketiminato (nacnac; **4**), 2-pyrrolylaldehyde (PyrAld; **5**), *N*-isopropyl-2-pyrrolylaldiminato (PyrIm^{IPr}; **6a**), *N*-ethyl-2-pyrrolylaldiminato (PyrIm^{Et}; **6b**), and *N*-isopropyl-2-salicylaldiminato (IPSA; **7**)} were investigated, and most combinations were found to deposit metal films or metal powder at 50 °C or less. SEM and XPS of metal films deposited on ruthenium showed a range of morphologies and compositions, including pure copper (excluding oxygen content after atmospheric exposure). These nonaqueous solution screening studies provided a rapid and convenient means to identify the most promising [Cu^{II}L₂] precursor/ER_{*n*} co-reagent combinations for copper metal ALD/pulsed-CVD studies, and subsequent ALD/pulsed-CVD studies were performed using **6b** in combination with AlMe₃, BEt₃ and ZnEt₂. As in solution, the reactivity of these reagents (pulsed-CVD) followed the order ZnEt₂ \approx AlMe₃ \gg BEt₃. Furthermore, at 120–150 °C, ZnEt₂ was used successfully to deposit smooth, conductive films composed of copper with 8–15% Zn. On the basis of CVD studies with ZnEt₂, zinc content appears to derive from a parasitic CVD process, which becomes more favorable above 120 °C, detracting from the goal of self-limiting deposition.

Introduction

Ultrathin metal films have a wide variety of applications in integrated circuits, magnetic information storage, fuel cells and catalysis. Copper, which is the focus of this work, has now replaced aluminum as the primary interconnect metal for most microelectronics applications, largely because of improvements in reliability, speed and scalability that result from lower resistivity and increased resistance to electromigration.^{1,2} Because interconnect metals must be deposited into high aspect ratio holes and trenches with ever decreasing top dimensions, highly conformal copper deposition is required in order to ensure complete filling of these features. Processes that have been used to deposit ultrathin copper films or copper seed layers include physical vapor deposition (PVD), chemical vapor deposition (CVD), electrodeposition (typically onto a pre-existing conformal copper seed layer) and electroless

deposition.^{1,3} However, all of these approaches face increasing challenges in terms of conformality and uniformity as critical dimensions decrease and aspect ratios increase,⁴ so new processes to allow more uniform and conformal copper metal deposition will likely be required.⁵

The process of atomic layer deposition (ALD), also referred to as atomic layer epitaxy (ALE), is a particularly promising method for the deposition of highly conformal, uniform thickness, ultrathin films of the type required in future microelectronics devices. ALD is related to the process of CVD, in that the metal source is a volatile metal complex. However, deposition is achieved not by thermal decomposition of a metal complex on a heated substrate surface (CVD), but by repeated alternating surface controlled reactions between a metal precursor and a co-reactant, at least one of which is adsorbed on the substrate surface during the nucleation process to initiate ALD film growth.

In a typical ALD process, the metal precursor is chemisorbed on the film surface in a self-limiting fashion (at a temperature at which CVD does not occur), and any excess precursor and volatile byproducts are removed with an inert gas purge. Vapors of a volatile co-reagent

*Corresponding author. (1) Fax: (905)-522-2509. Tel: (905)-525-9140, x23307. E-mail: emslied@mcmaster.ca (D.J.H.E.); (2) E-mail: scott.b.clendenning@intel.com (S.B.C.).

(1) Rosenberg, R.; Edelstein, D. C.; Hu, C.-K.; Rodbell, K. P. *Annu. Rev. Mater. Sci.* **2000**, *30*, 229.
(2) Hau-Riege, C. S. *Microelectron. Reliab.* **2004**, *44*, 195.
(3) (a) Kim, H. *Surf. Coat. Technol.* **2006**, *200*, 3104. (b) Carraro, C.; Maboudian, R.; Magagnin, L. *Surf. Sci. Rep.* **2007**, *62*, 499. (c) Shacham-Diamand, Y.; Inberg, A.; Sverdllov, Y.; Bogush, V.; Croitoru, N.; Moscovich, H.; Freeman, A. *Electrochim. Acta* **2003**, *48*, 2987.

(4) *The International Technology Roadmap for Semiconductors 2007*; Semiconductor Industry Association: San Jose, CA, 2007; <http://www.itrs.net/>.

(5) Kim, H. J. *Vac. Sci. Technol., B* **2003**, *21*, 2231.

(e.g., H₂, O₂, H₂O, H₂S, or NH₃) are then introduced to the surface, and react with the chemisorbed metal precursor to deposit the desired material (e.g., a metal or metal oxide film), effect the release of volatile byproducts, and create a suitable surface functionalization to allow reaction in the next metal precursor vapor exposure. The surface reaction with the co-reagent is also self-limiting and excess co-reagent and volatile byproducts are removed with an inert gas purge. In this fashion, so long as sufficient vapor doses of the metal precursor and co-reagent are delivered to ensure maximum surface coverage

and complete reaction, the film thickness will depend only on the number of precursor/purge/co-reagent/purge cycles, and the film will grow conformally on all exposed surfaces on which nucleation can occur. If self-limiting behavior cannot be achieved (even in cases where ALD reactivity is accompanied by a minor parasitic CVD process), the overall process is termed pulsed-CVD, although the experimental setup is identical to that for ALD.^{5–7}

The material deposited in ALD is typically elemental metal with H₂ or O₂ (only in the case of noble metals such as Rh, Ir, Pd, Pt),⁵ a metal oxide with H₂O or O₃,^{7,8} a metal nitride with NH₃ or RNH₂,⁵ a metal sulphide with H₂S,⁹ and a metal selenide or telluride with H₂Se, Se-(SiR₃)₂, or Te(SiR₃)₂.^{10,11} However, although ALD of a wide range of metal oxides and nitrides has been demonstrated, ALD of metals is far less common (see Table S1 in Supporting Information).^{12–22} One reason for this is the very limited selection of co-reagents currently available for ALD of metal films. In addition, the strongly reducing or oxidizing nature of these reagents (especially at high temperatures) significantly limits the range of substrates compatible with metal ALD. Further, the requirement for high temperatures (typically 200–400 °C) precludes the use of metal ALD on many less thermally robust substrates, has the potential to cause dewetting leading to discontinuous films,^{23,24} and greatly reduces the number of suitable metal precursors, because thermal decomposition leading to CVD rather than ALD must be avoided.

For thermal copper metal ALD, initial reports involved H₂ in combination with CuCl at 360–410 °C,²¹ [Cu(thd)₂] (thd = 2,2,6,6-tetramethyl-3,5-heptanedionate) at 190–260 °C,²⁰ and [Cu(acac)₂] at 250 °C.¹⁹ More recently, Gordon et al. reported the use of a liquid copper amidinate precursor, [Cu₂{(tBuN)₂CMe}₂], which allowed ALD with H₂ at temperatures in the range 150–190 °C,¹³ much lower than achieved with [Cu₂{(PrN)₂CMe}₂] (280 °C).^{17,18} Plasma-enhanced ALD (PEALD)²⁵ has also been investigated for metal deposition, but this technique requires more complex ALD reactors, is often considered less suitable for deposition on substrates with high-aspect-ratio features because of rapid recombination of radical species, and can lead to substrate surface damage.^{5,17} In addition, indirect approaches to metal ALD have been reported, including ALD of Cu₃N followed by conversion to copper metal by treatment with H₂ at 160 °C,²⁶ and ALD of CuO followed by conversion to copper metal, either electrochemically in an aqueous solution of a metal hydroxide,

- (6) (a) Leskelä, M.; Ritala, M. *Angew. Chem., Int. Ed.* **2003**, *42*, 5548. (b) Leskelä, M.; Niinistö, L.; Pakkanen, T.; Mason, N. J.; Tischler, M. A.; Bedair, S. M.; Yao, T. In *Atomic Layer Epitaxy*; Suntola, T., Simpson, M., Eds.; Blackie: Glasgow, 1990. (c) Ritala, M.; Leskelä, M. *Atomic Layer Deposition*. In *Handbook of Thin Film Materials*; Nalwa, H. S., Ed.; Academic Press: San Diego, 2001; Vol. 1 – Deposition and Processing of Thin Films, p 103. (d) Zaera, F. J. *Water. Chem.* **2008**, *18*, 3521. (e) Kim, H.; Lee, H.-B.-R.; Maeng, W.-J. *Thin Solid Films* **2009**, *517*, 2563. (f) Knez, M.; Nielsch, K.; Niinistö, L. *Adv. Mater.* **2007**, *19*, 3425.
- (7) Niinistö, L.; Päiväsaari, J.; Niinistö, J.; Putkonen, M.; Nieminen, M. *Phys. Status Solidi A* **2004**, *201*, 1443.
- (8) Hämäläinen, J.; Kemell, M.; Munnik, F.; Kreissig, U.; Ritala, M.; Leskelä, M. *Chem. Mater.* **2008**, *20*, 2903.
- (9) Pore, V.; Ritala, M.; Leskelä, M. *Chem. Vap. Deposition* **2007**, *13*, 163 and references therein.
- (10) (a) Pore, V.; Hatanpää, T.; Ritala, M.; Leskelä, M. *J. Am. Chem. Soc.* **2009**, *131*, 3478 and references therein. (b) Knapas, K.; Hatanpää, T.; Ritala, M.; Leskelä, M. *Chem. Mater.* **2010**, *22*, 1386.
- (11) Thermal ALD of various other classes of material have also been reported, for example arsenides and phosphides (e.g., AlAs, GaAs and InP).
- (12) Lee, B. H.; Hwang, J. K.; Nam, J. W.; Lee, S. U.; Kim, J. T.; Koo, S.-M.; Baunemann, A.; Fischer, R. A.; Sung, M. M. *Angew. Chem., Int. Ed.* **2009**, *48*, 4536.
- (13) (a) Li, Z.; Rahtu, A.; Gordon, R. G. *J. Electrochem. Soc.* **2006**, *153*, C787. (b) Li, Z.; Barry, S. T.; Gordon, R. G. *Inorg. Chem.* **2005**, *44*, 1728.
- (14) Park, K.-H.; Bradley, A. Z.; Thompson, J. S.; Marshall, W. J. *Inorg. Chem.* **2006**, *45*, 8480.
- (15) Park, K.-H.; Marshall, W. J. *J. Am. Chem. Soc.* **2005**, *127*, 9330.
- (16) Grushin, V. V.; Marshall, W. J. *Adv. Synth. Catal.* **2004**, *346*, 1457.
- (17) Lim, B. S.; Rahtu, A.; Gordon, R. G. *Nat. Mater.* **2003**, *2*, 749.
- (18) Lim, B. S.; Rahtu, A.; Park, J.-S.; Gordon, R. G. *Inorg. Chem.* **2003**, *42*, 7951.
- (19) Urtiainen, M.; Kröger-Laukkanen, M.; Johansson, L.-S.; Niinistö, L. *Appl. Surf. Sci.* **2000**, *157*, 151.
- (20) Mårtensson, P.; Carlsson, J.-O. *J. Electrochem. Soc.* **1998**, *145*, 2926.
- (21) Mårtensson, P.; Carlsson, J.-O. *Chem. Vap. Deposition* **1997**, *3*, 45.
- (22) (a) Goldstein, D. N.; George, S. M. *Appl. Phys. Lett.* **2009**, *95*, 143106. (b) Kim, S.-W.; Kwon, S.-H.; Kwak, D.-K.; Kang, S.-W. *J. Appl. Phys.* **2008**, *103*, 023517. (c) Hämäläinen, J.; Munnik, F.; Ritala, M.; Leskelä, M. *Chem. Mater.* **2008**, *20*, 6840. (d) Ten Eyck, G. A.; Pimanpong, S.; Bakhrui, H.; Lu, T.-M.; Wang, G.-C. *Chem. Vap. Deposition* **2006**, *12*, 290. (e) Aaltonen, T.; Ritala, M.; Leskelä, M. *Electrochem. Solid-State Lett.* **2005**, *8*, C99. (f) Aaltonen, T.; Ritala, M.; Sammelselg, V.; Leskelä, M. *J. Electrochem. Soc.* **2004**, *151*, G489. (g) Aaltonen, T.; Ritala, M.; Tung, Y.-L.; Chi, Y.; Arstila, K.; Meinander, K.; Leskelä, M. *J. Mater. Res.* **2004**, *19*, 3353. (h) Aaltonen, T.; Ritala, M.; Sajavaara, T.; Keinonen, J.; Leskelä, M. *Chem. Mater.* **2003**, *15*, 1924. (i) Aaltonen, T.; Ritala, M.; Arstila, K.; Keinonen, J.; Leskelä, M. *Chem. Vap. Deposition* **2004**, *10*, 215. (j) Aaltonen, T.; Alén, P.; Ritala, M.; Leskelä, M. *Chem. Vap. Deposition* **2003**, *9*, 45. (k) Senkevich, J. J.; Tang, F.; Rogers, D.; Drotar, J. T.; Jezewski, C.; Lanford, W. A.; Wang, G.-C.; Lu, T.-M. *Chem. Vap. Deposition* **2003**, *9*, 258. (l) Min, Y.-S.; Bae, E. J.; Jeong, K. S.; Cho, Y. J.; Lee, J.-H.; Choi, W. B.; Park, G.-S. *Adv. Mater.* **2003**, *15*, 1019. (m) Kim, S. H.; Hwang, E. S.; Kim, B. M.; Lee, J. W.; Sun, H. J.; Hong, T. E.; Kim, J. K.; Sohn, H.; Kim, J.; Yoon, T. S. *Electrochem. Solid-State Lett.* **2005**, *8*, C155. (n) Kim, S. H.; Kwak, N.; Kim, J.; Sohn, H. *J. Electrochem. Soc.* **2006**, *153*, G887 and references therein. (o) Klaus, J. W.; Ferro, S. J.; George, S. M. *Thin Solid Films* **2000**, *360*, 145. (p) Grubbs, R. K.; Steinmetz, N. J.; George, S. M. *J. Vac. Sci. Technol., B* **2004**, *22*, 1811.
- (23) Wu, L.; Eisenbraun, E. *Electrochem. Solid-State Lett.* **2008**, *11*, H107.
- (24) (a) Han, B.; Wu, J.; Zhou, C.; Li, J.; Lei, X.; Norman, J. A. T.; Gaffney, T. R.; Gordon, R.; Roberts, D. A.; Cheng, H. *J. Phys. Chem. C* **2008**, *112*, 9798. (b) Wu, J.; Han, B.; Zhou, C.; Lei, X.; Gaffney, T. R.; Norman, J. A. T.; Li, Z.; Gordon, R.; Cheng, H. *J. Phys. Chem. C* **2007**, *111*, 9403.
- (25) An alternative approach that has been used successfully to effect ALD of various metals (e.g., Ta, Ti, Al, Co, and Cu) at lower temperatures is the use of plasma to generate radicals (e.g., atomic hydrogen) from co-reagents such as H₂ and NH₃. This technique is referred to as radical-enhanced ALD (REALD) or plasma-enhanced ALD (PEALD) (see ref 5).
- (26) Li, Z.; Gordon, R. G. *Chem. Vap. Deposition* **2006**, *12*, 435.

or by treatment with reagents such as H₂ (270–320 °C), H-plasma (150–300 °C), CO, ROH, formalin, RCHO, or RCO₂H.²⁷

Deposition of copper metal at temperatures well below 200 °C has been reported using copper(I)^{14,28} or copper(II)^{15,29} β-diketiminato precursors in combination with H₂SiEt₂, both in solution and by exposure of films of the copper complexes to diethylsilane.³⁰ However, the effectiveness of this co-reagent (and the temperatures that would be required) to effect copper metal deposition from the copper(II) precursors under realistic ALD conditions was not disclosed, and a recent report has demonstrated a pulsed-CVD mechanism, rather than an ALD mechanism, for copper deposition using [(nacnac)Cu(H₂C=CHSiMe₃)] {nacnac = (CH₂)₃N–C=CH–CMe=NH} with H₂SiEt₂.³¹ Proof-of-concept studies on copper film deposition using copper(II) pyrrolylaldimine complexes with H₂SiEt₂ (160–170 °C) or a 1:1 mixture of H₂ and NH₃ (≥ 180 °C) have also been described.¹⁶ Additionally, copper metal (containing 5–16% carbon) deposition at temperatures between 25 and 100 °C was recently reported using sequential pulses of [Cu(hfac)₂], pyridine and H₂. Pyridine is proposed to interact with surface-bound Cu(hfac)₂ to weaken the Cu–O bonds and facilitate reduction by H₂. However, self-limiting film growth was not reported.³² The most prominent example of low-temperature copper metal ALD was published during the course of this work by Sung and Fischer et al., and involves reaction of bis(*N,N*-dimethyl-2-aminoisopropoxide)copper(II) with ZnEt₂ at 100–120 °C. Copper films were deposited: (a) on oxidized Si(100) substrates with a growth rate of 0.2 Å/cycle, (b) on an oxidized silicon substrate patterned with alkyl siloxane SAMs, and (c) inside the pores of a nanoporous polycarbonate membrane, providing copper nanotubes after treatment with chloroform.¹² This work marks the emergence of a new class of co-reagent for late transition metal ALD.

Herein we report the use of solution deposition studies as a means to identify particularly promising metal precursor/co-reagent combinations for metal ALD or pulsed-CVD. These studies are rapid and straightforward, unlike ALD/pulsed-CVD studies, which are time-consuming, resource intensive, and require the use of highly specialized equipment. Co-reagents investigated in this work are AlMe₃, BEt₃, and ZnEt₂, and studies into the potential of these co-reagents for copper metal ALD/pulsed-CVD are described.

Results and Discussion

Co-Reagent Selection. The homoleptic alkyl compounds AlMe₃, BEt₃, and ZnEt₂ were investigated as co-reagents to allow copper metal ALD/pulsed-CVD under mild conditions (low temperatures (100–200 °C) and the absence of strong, unselective reducing or oxidizing agents). Their Lewis acidity, compatibility with hard N- and O-donor ligands, and alkylating ability makes them excellent candidates to convert CuL₂ precursors to “LCuR”, “CuR₂”, and/or “CuR” (R = Me, Et, or H) complexes, which can be expected to undergo facile decomposition leading to copper metal; detailed investigations into the pathways responsible for solution-deposition of copper metal are described in the subsequent companion article.³³ The co-reagents AlMe₃, BEt₃, and ZnEt₂ are also inexpensive, thermally stable, volatile, and liquid at room temperature,³⁴ so are readily deliverable in an ALD or pulsed-CVD process. Furthermore, they are expected to be more selective in the initiation of reduction processes than H₂ or compounds containing E–H (E = B, Al, Si, etc.) bonds, and the use of liquid, rather than gaseous co-reagents allows solution screening studies to be performed in an efficient semi-combinatorial fashion (inside an inert-atmosphere workstation), prior to ALD/pulsed-CVD studies.

Copper Precursor Complexes. All copper precursors investigated in this work are of the form [Cu^{II}L₂], where L is acetylacetonate (acac; **1**),³⁵ hexafluoroacetylacetonate (hfac; **2**),^{36,37} *N*-isopropyl-β-ketiminato (acnac; **3**), *N,N*-dimethyl-β-diketiminato (nacnac; **4**),^{15,38} 2-pyrrolylaldehyde (PyrAld; **5**),³⁹ *N*-isopropyl-2-pyrrolylaldimine (PyrIm^{iPr}; **6a**), *N*-ethyl-2-pyrrolylaldimine (PyrIm^{Et}; **6b**),^{16,40} and *N*-isopropyl-2-salicylaldimine (IPSA; **7**)^{41,42} (Figure 1). Complexes **1**³⁵ and **2**^{37,43} are square planar, whereas **7**⁴² deviates toward tetrahedral geometry with an interligand angle of 59 degrees. The solid-state structures of **4**, **6a**, and **6b** have not been reported. However, based on related structures in the literature (see the Supporting Information, Table S1), and bearing in mind that more effective electron donation and increased steric hindrance have been reported to result in greater distortion toward

- (27) (a) Soininen, P. J.; Elers, K.-E.; Haukka, S. U.S. Patent 6 482 740 B2, 2002. Kostamo, J.; Stokhof, M. U.S. Patent 7 067 407 B2, 2006. (b) Huo, J.; Solanki, R.; McAndrew, J. J. *Mater. Res.* **2002**, *17*, 2394. (c) Solanki, R.; Pathangey, B. *Electrochem. Solid-State Lett.* **2000**, *3*, 479.
- (28) Bradley, A. Z.; Thompson, J. S. World Patent WO 094689 A2, 2004.
- (29) Bradley, A. Z.; Thorn, D. L.; Thompson, J. S. World Patent WO 095701 A1, 2003.
- (30) Other reagents including BBN, B₂H₆, BR_xH_(3-x), dihydrobenzofuran, pyrazoline, disilane, SiH₄, SiR_xH_(4-x), and GeR_xH_(4-x) are also mentioned in refs 28 and 29.
- (31) Thompson, J. S.; Zhang, L.; Wyre, J. P.; Brill, D. J.; Lloyd, K. G. *Thin Solid Films* **2009**, *517*, 2845.
- (32) Kang, S.-W.; Yun, J.-Y.; Chang, Y. H. *Chem. Mater.* **2010**, *22*, 1607.

- (33) Vidjayacoumar, B.; Emslie, D. J. H.; Blackwell, J. M.; Clendenning, S. B.; Britten, J. F. *Chem. Mater.* **2010**, DOI:10.1021/cm101443x.
- (34) AlMe₃ (bp 125 °C) was selected, rather than AlEt₃ (bp 186 °C), due to the greatly reduced cost of pure material and a lower boiling point. Liquid BEt₃ (bp 95 °C) was used, rather than gaseous BMe₃ (bp –20 °C), for more straightforward handling. ZnEt₂ (bp 117 °C) was also selected, rather than ZnMe₂ (bp 45 °C), for more straightforward handling.
- (35) Lebrun, P. C.; Lyon, W. D.; Kuska, H. A. J. *Crystallogr. Spectrosc. Res.* **1986**, *16*, 889.
- (36) (a) Bertrand, J. A.; Kaplan, R. I. *Inorg. Chem.* **1966**, *5*, 489. (b) Funck, L. L.; Ortolano, T. R. *Inorg. Chem.* **1968**, *7*, 567.
- (37) Maverick, A. W.; Fronczek, F. R.; Maverick, E. F.; Billodeaux, D. R.; Cygan, Z. T.; Isovitsch, R. A. *Inorg. Chem.* **2002**, *41*, 6488.
- (38) McGeachin, S. G. *Can. J. Chem.* **1968**, *46*, 1903.
- (39) Perry, C. L.; Weber, J. H. *J. Inorg. Nucl. Chem.* **1971**, *33*, 1031.
- (40) (a) Holm, R. H.; Chakravorty, A.; Theriot, L. J. *Inorg. Chem.* **1966**, *5*, 625. (b) Yokoi, H.; Addison, A. W. *Inorg. Chem.* **1977**, *16*, 1341.
- (41) Sacconi, L.; Ciampolini, M. *J. Chem. Soc.* **1964**, 267.
- (42) Orioli, P. L.; Sacconi, L. *J. Am. Chem. Soc.* **1966**, *88*, 277.
- (43) Pinkas, J.; Huffman, J. C.; Bollinger, J. C.; Streib, W. E.; Baxter, D. V.; Chisholm, M. H.; Caulton, K. G. *Inorg. Chem.* **1997**, *36*, 2930.

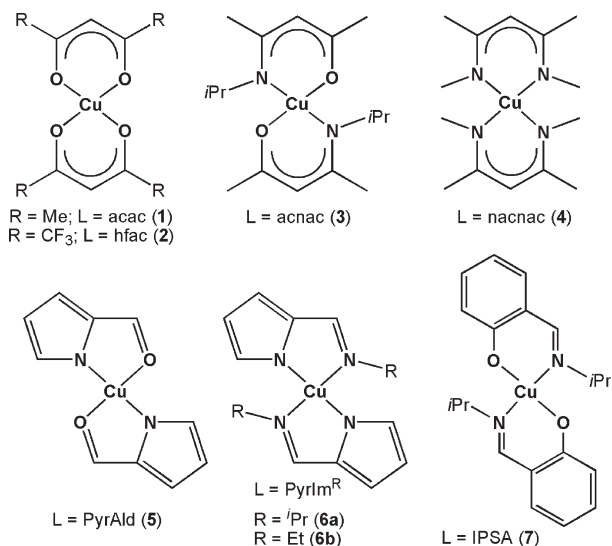


Figure 1. Homoleptic copper(II) complexes 1–7.

tetrahedral geometry in [CuL₂] (L = 2-pyrrolyaldimine) complexes,¹⁶ interligand tilt angles of ~60° for **4**,¹⁵ 45–55° for **6a**, and 40–45° for **6b**.^{16,44} can be expected.

X-ray quality crystals of **3** were obtained from hexanes at –30 °C, and confirmed that the complex is 4-coordinate,⁴⁵ with an interligand tilt angle of 59° (Figure 2). The Cu–O bond distance of 1.916(1) Å is similar to those observed in [Cu(acac)₂] (**1**) [1.912(4) and 1.914(4) Å],³⁵ and the Cu–N bond distance of 1.974(2) Å is only slightly longer than those observed in [CuL₂] (L = *N*-methyl-*N'*-ethyl-β-diketiminato; Cu–N 1.93–1.95 Å).¹⁵ X-ray quality crystals of **5** were prepared by slow evaporation of a diethyl ether solution at room temperature. Complex **5** is square planar, as are **1** and **2**, which are similarly free from unfavorable interligand steric interactions (Figure 3). The anionic N-donors in **5** are *trans*-disposed, and the Cu–N bond distance [1.918(2) Å] is slightly shorter than those typically observed for pyrrolyaldimine complexes (1.93–1.96 Å).¹⁶

Complexes 1–7 were selected because of ease of synthesis, reasonable thermal stability and volatility (in most cases), and for **1**, **2**, and **4**, reported use in copper metal CVD and/or ALD. They also represent a variety of different ligand types, differing in donor-set, the extent

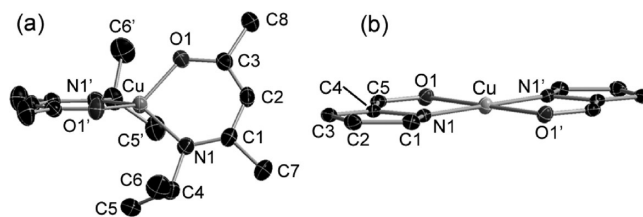


Figure 2. Solid-state structure of complexes (a) **3** and (b) **5** with thermal ellipsoids at 50%. Hydrogen atoms are omitted for clarity.

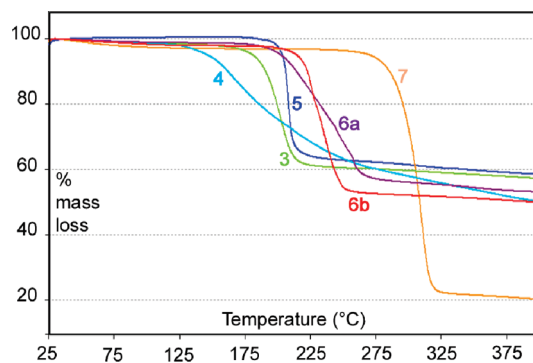


Figure 3. Thermogravimetric analyses (TGA) for complexes 3–7 under an argon atmosphere. The temperature was increased at a rate of 10 °C/min.

of electron delocalization, and steric/electronic properties. Thermogravimetric analyses (TGA) for the less well-studied complexes in the group (3–7) are shown in Figure 3; it is believed that weight loss is primarily due to decomposition with volatilization of the organic by-products and not vaporization of the copper complex itself, with the possible exception of complex **7**. The most thermally robust precursor is **7** and the least robust is **4**, with all other complexes showing an onset of decomposition at 170–220 °C. Under a vacuum of 1×10^{-2} Torr, sublimation temperatures for the complexes studied were 120 °C for **1**, < 20 °C for **2**, 80 °C for **3**, 80 °C (with accompanying decomposition) for **4**, 120 °C for **6a**, 90 °C for **6b**, and 120 °C for **7** (complex **5** was not volatile).

Solution Screening Studies. Our approach to the development of new low-temperature methods for copper metal ALD/pulsed-CVD focused on the initial application of nonaqueous solution screening experiments. These experiments could be conducted rapidly and in parallel, with visual identification of metal film and metal powder deposition and subsequent analysis by SEM, XPS, and/or PXRD to confirm that deposited material was largely composed of copper. This approach provided an efficient and straightforward means to probe the extent to which the primary steps for copper metal deposition occur in the temperature range most relevant to new low-temperature ALD/pulsed-CVD method development (25–120 °C), and to determine the most promising copper precursor/co-reagent combinations for subsequent ALD/pulsed-CVD studies. Solution reactions also provide a valuable opportunity for detailed mechanistic studies using a range of powerful and readily accessible characterization techniques,⁴⁶ and the pathways responsible for copper metal deposition in the solution reactions of **6a** with

(44) (a) Wei, C. H. *Inorg. Chem.* **1972**, *11*, 2315. (b) Wansapura, C. M.; Choi, J. Y.; Simpson, J. L.; Szymanski, D.; Eaton, G. R.; Eaton, S. S.; Fox, S. *J. Coord. Chem.* **2003**, *56*, 975.

(45) Complex **3** is red-brown with a λ_{max} of 470 nm ($\epsilon = 870 \text{ L mol}^{-1} \text{ cm}^{-1}$), which is an unusually low wavelength absorption for a copper(II) complex, and is also unexpected given literature reports for related [Cu(acnac)₂] compounds: the *N*-methyl analogue is reported to be a grey powder or dark green crystals, the *N*-CH₂OMe analogue is dark green-black, the *N*-Ph analogue is black, and the *N*-2,6-diisopropylphenyl derivative is dark green. Given the paramagnetic nature of **3** ($\mu_{\text{eff}} 1.91 \mu_{\text{B}}$ at 24 °C), the solid-state structure was determined in order to verify the identity of the complex. (a) Holtzclaw, H. F., Jr.; Collman, J. P.; Alire, R. M. *J. Am. Chem. Soc.* **1958**, *80*, 1100. (b) Baidina, I. A.; Stabnikov, P. A.; Vasiliev, A. D.; Gromilov, S. A.; Igumenov, I. K. *J. Struct. Chem.* **2004**, *45*, 671. (c) Baxter, D. V.; Caulton, K. G.; Chiang, W.-C.; Chisholm, M. H.; DiStasi, V. F.; Dutremez, S. G.; Folting, K. *Polyhedron* **2001**, *20*, 2589. (d) Hsu, S. H.; Li, C. Y.; Chiu, Y. W.; Chiu, M. C.; Lien, Y. L.; Kuo, P. C.; Lee, H. M.; Huang, J. H.; Cheng, C. P. *J. Organomet. Chem.* **2007**, *692*, 5421.

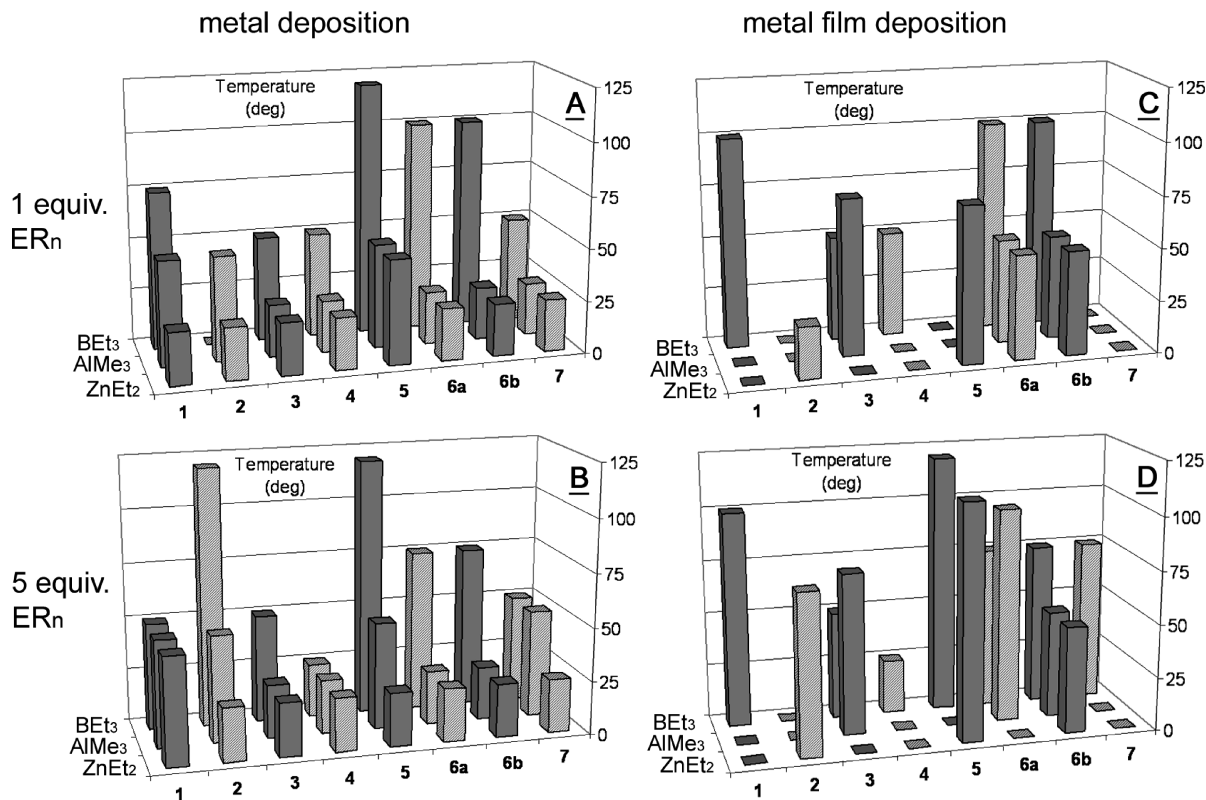


Figure 4. Minimum temperatures for (A, B) deposition of a copper-containing film and/or powder, and (C, D) deposition of a copper-containing film.⁴⁷ Graphs A and C correspond to 1:1 reactions of complexes 1–7 with AlMe₃, BEt₃, and ZnEt₂, whereas graphs B and D correspond to reactions with 1:5 stoichiometry. Solutions were 13.6 mM (1.1 mL total volume; A and C) or 10 mM (1.5 mL total volume; B and D) in copper complex, and reactions were maintained for 24 h at each of the following temperatures in sequence: 25, 50, 75, 100, 120 °C. The x-axis refers to metal complex (1–7), the y-axis (vertical) refers to deposition temperature, and the z-axis indicates the co-reagent employed (BEt₃, AlMe₃, or ZnEt₂). Bars at the baseline on the graphs correspond to complexes that did not deposit metal (graphs A and B) or a metal film (graphs C and D) within the temperature range studied.

AlMe₃, BEt₃ and ZnEt₂ are discussed in a subsequent companion article.³³

Solution screening studies were performed by maintaining toluene solutions of 1–7 with AlMe₃, BEt₃ or ZnEt₂ (1 and 5 equiv) for 24 h at each of the following temperatures in sequence: 25, 50, 75, 100, and 120 °C. Deposition of either a copper-colored metal film or precipitation of a black or copper-colored powder was observed at 25–50 °C in >85% of the reactions (Figure 4), and in some cases, solution color changes were observed at 25 °C, prior to metal deposition. The latter observation indicates disappearance of [CuL₂] prior to rather than concurrent with metal deposition. For example, addition of AlMe₃ and ZnEt₂ to 6a led to immediate consumption of the copper-

(II) precursor, even at –78 °C, although significant copper metal deposition was not observed until the temperature was raised to –20 °C for ZnEt₂ and 20 °C for AlMe₃.⁴⁸ In contrast to the high observed reactivity of the organoaluminum and zinc reagents, BEt₃ reacted only slowly with 1–7, even at 50 to 75 °C.

Metal powders deposited in the reactions of 1–7 with AlMe₃, BEt₃, and ZnEt₂ were shown to be composed of copper (within the limits of detection by PXRD, which does not include amorphous materials), with the exception of that from 7 with ZnEt₂, which was identified as mixture of amorphous Zn (84%) and brass (β -CuZn;16%)⁴⁹ by a combination of PXRD and XPS.⁵⁰ Metal precursor/ER_n co-reagent reactions resulting in the formation of a metal film (7 combinations using BEt₃, 3 with AlMe₃, and 4 with ZnEt₂) were repeated in the presence of Si/SiO₂/Ta/Ru wafer sections, and the resulting films were analyzed by XPS after initial sputtering to remove higher levels of oxidized material and organic impurities at the surface.

(46) The elucidation of ALD mechanisms faces many challenges because of the metrology restrictions placed on chemical analysis inside an ALD reactor as well as the very small quantities of surface species and vapor-phase byproducts. The ability to monitor solution-based reactivity between a metal precursor and co-reagent by standard techniques including NMR spectroscopy and X-ray crystallography may offer a powerful approach to gain insight into the mechanisms behind atomic layer deposition processes, especially those occurring at low temperatures (e.g., <150 °C).

(47) Successful metal deposition is reported in Figure 4 only when a significant quantity of copper was deposited by visual inspection. Given that each reaction involved only 4–6 mg (15 μ mol) of the copper precursor, this corresponds to deposition of a substantial percentage of the copper metal present.

(48) Both AlMe₃ and ZnEt₂ reacted with 6a within seconds at –78 °C. However, the rate of copper deposition was determined by the thermal stability of the copper(I) alkyl complex, [CuR]_n, that formed en route to copper metal (see ref 33).

(49) Shimizu, S.; Murakami, Y.; Kachi, S. *J. Phys. Soc. Jpn.* **1976**, *41*, 79.

(50) Colloidal brass (5–65 at % Zn in Cu) has been prepared either by addition of an octylamine solution of [Cu(OCHMeCH₂NMe₂)₂] and ZnEt₂ to hexadecylamine at 250 °C, or by sequential addition of octylamine solutions of [Cu(OCHMeCH₂NMe₂)₂] and then ZnEt₂ to hexadecylamine at 250 °C. Pure colloidal copper and zinc were also accessible by addition of an octylamine solution of just [Cu(OCHMeCH₂NMe₂)₂] or ZnEt₂ to hexadecylamine at 250 °C: Hambrock, J.; Schröter, M. K.; Birkner, A.; Wöll, C.; Fischer, R. A. *Chem. Mater.* **2003**, *15*, 4217.

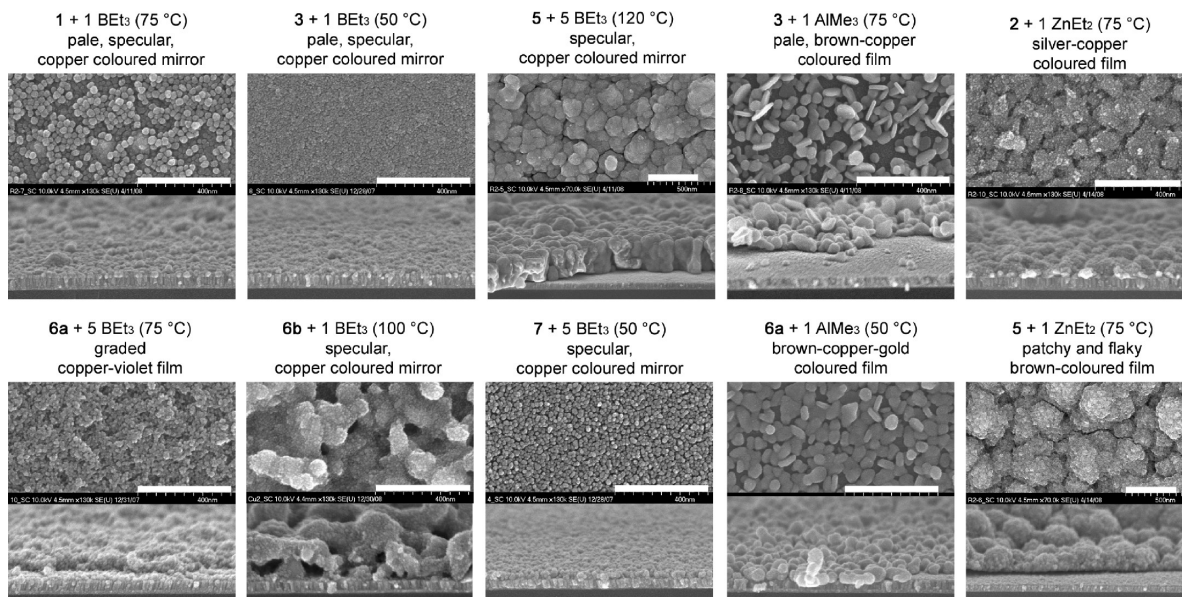


Figure 5. SEM images of selected metal films deposited on ruthenium through the reactions of **1–7** with ER_n co-reagents in toluene (SEM images for the film deposited through the reaction of **6b** with $ZnEt_2$ in toluene are shown in Figure 6). For each film, the reagents, reaction stoichiometry, reaction temperature, and macroscopic film appearance is provided. White scale bars are set to 400 nm.

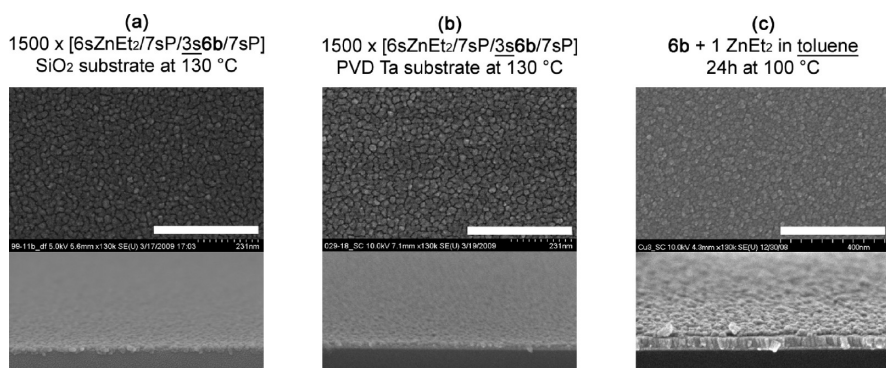


Figure 6. (a, b) SEM images of films deposited at 130 °C on SiO_2 and PVD Ta, respectively, using 1500 cycles of: 6 s pulse $ZnEt_2$ /7s chamber purge/3s pulse of **6b**/7s chamber purge. (c) SEM image of the film deposited on PVD Ru through the reaction of **6b** with 1 equiv. of $ZnEt_2$ in toluene at 100 °C for 24 h. In figure captions, s = seconds and P = purge. White scale bars are set to 400 nm.

SEM images for a selection of the films are provided in Figure 5, and elemental composition (by XPS) is provided in the Supporting Information. These data are of independent interest from the perspective of metal film solution deposition, and an understanding of film morphology is also valuable for the interpretation of XPS data. However, the morphology of solution-deposited films is not expected to correlate with film morphologies observed by ALD or pulsed-CVD. Key findings were: (1) All but one film showed good adhesion to the substrate, as determined by a standard tape test. (2) Films were 10–300 nm thick and of varied morphology; from dense solid films with an undulating surface, to continuous films of densely packed approximately spherical 5–35 nm grains, to a loosely packed layer of 30–130 nm diameter platelet-shaped granules (Figure 5). (3) Copper films deposited using BEt_3 contained very low levels of boron (0–1.5 at%) and did not contain nitrogen at levels detectable by XPS (~0.5 at %). (4) Metal films deposited using $AlMe_3$ contained <0.5 at % N, but significant amounts of Al; from 8 to 42%

Al in Cu. (5) Films deposited using $ZnEt_2$ contained varying amounts of Zn, with compositions ranging from 2.5% Zn in Cu, to predominantly Zn. (6) As is typically observed after exposure to the atmosphere, oxygen was present in all films (typically 2–10 at % relative to Cu), including those prepared from oxygen-free precursors (complexes **4** and **6**).⁵¹ (7) Carbon was present in many of the films (e.g., 0–5% in films deposited using BEt_3 or $AlMe_3$). (8) The amount of oxygen and carbon in the films varied greatly depending on the amount of B, Al, or Zn incorporated in the film, the susceptibility of each element to oxidation ($Al > Zn > B$), the nature of the ligands in $[CuL_2]$, film thickness, and film morphology (e.g., porosity, grain size and surface coverage).

These screening studies demonstrate the potential utility of $AlMe_3$, BEt_3 , and $ZnEt_2$ as new co-reagents for

(51) Repeating XPS measurements on several freshly prepared films (from BEt_3 with **1**, **6**, and **7**) that had been exposed to air for 5–10 min, rather than 2 weeks, did not show significantly lower levels of oxygen or carbon.

low-temperature copper metal ALD or pulsed-CVD, and also the suitability of copper(II) complexes as precursors for copper deposition (see below for ALD/pulsed-CVD studies using AlMe_3 , BEt_3 , and ZnEt_2 in combination with complex **6b**). Copper(II) precursors are often considered less reactive than copper(I) precursors, but in many cases offer the advantages of straightforward preparation, modification, and handling (many are air stable), and higher thermal stability. These studies also highlight the sensitivity of Cu film composition to the nature of the ligands in the $[\text{CuL}_2]$ precursor and the choice of ER_n co-reagent. However, it is important to note that while in solution, films with lower B, Al, or Zn content require the formation of soluble and thermally robust B, Al, and Zn byproducts, in metal ALD, byproduct volatility and thermal stability are key factors in determining the level of B, Al, or Zn incorporation. That said, the potential benefits of alloying elements for copper interconnect applications were recently discussed; aluminum is listed in a group of 10 elements of particular interest (Pd, Au, Al, In, Ag, Cr, B, Ti, Nb, and Mn), whereas zinc is included in a list of an additional 6 elements worthy of further investigation (Zn, V, C, Mg, P, and Sn).⁵²

Copper Metal ALD/Pulsed-CVD Studies. Based on solution screening results as well as CuL_2 complex properties, the precursor complex bis(*N*-ethyl-2-pyrrolylaldimine)copper(II) (**6b**) was selected for ALD/pulsed-CVD evaluation with the co-reagents AlMe_3 , BEt_3 and ZnEt_2 . Desirable features of complex **6b** are volatility, the absence of oxygen or fluorine in the ligands, and good thermal stability; CVD was not observed in the temperature range of interest ($\leq 150^\circ\text{C}$).

Deposition Studies Using AlMe_3 and BEt_3 as Co-Reagents. At temperatures of $120\text{--}150^\circ\text{C}$ using **6b** with AlMe_3 as the co-reagent, copper-containing films were deposited via a pulsed-CVD mechanism. However, the resulting films were nonconductive and granular with a high Al and O content (after atmospheric exposure). The lack of electrical conductivity presumably stems from the presence of insulating Al_2O_3 (Al $2s$ binding energy of 119.0 eV). Because the ALD chamber received a two hour forming gas prebake at 250°C prior to ALD/pulsed-CVD processing, the most likely source of Al_2O_3 in the film is the oxidation of metallic Al upon film exposure to air. Similar results were obtained using complex **7** in combination with AlMe_3 . By contrast, no film was deposited when BEt_3 was used as a co-reagent with **6b** or **7**. The observation of deposition with AlMe_3 , but not BEt_3 , is in keeping with the order of reactivity observed in solution ($\text{AlMe}_3 \gg \text{BEt}_3$). However, factors such as ineffective chemisorption of BEt_3 vapors on the surface, or initial surface reactivity that does not result in the formation of active sites suitable to allow further film growth could also play an important role.

Deposition using ZnEt_2 as Co-Reagent. With ZnEt_2 in combination with **6b**, conductive copper films were

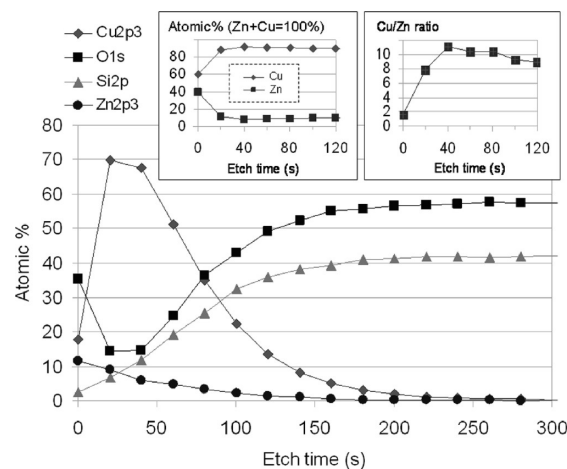


Figure 7. XPS determined atomic percent compositional depth profile [carbon values were <2 at % at all sputter depths (20–300 s), so are not included in the profile] of film deposited on SiO_2 at 130°C using 1500 cycles of the following pulse sequence: 6 s pulse ZnEt_2 /7 s chamber purge/3 s pulse of **6b**/7 s chamber purge. The inset on the left plots Zn at % and Cu at % where the total Zn and Cu content is set to 100%. The inset on the right plots the Cu:Zn ratio against etch time.

deposited from 120 to 150°C on SiO_2 , PVD Ta and PVD Ru substrates. All films are granular with low carbon impurities post sputter (<2 at %) and no detectable nitrogen, suggesting minimal incorporation of the *N*-ethyl-2-pyrrolylaldimine or ethyl ligands. In a typical deposition, a pulse sequence consisting of a 6 s pulse of ZnEt_2 followed by a 7 s chamber purge, a 3 s pulse of **6b**, and a final 7 s chamber purge yielded granular films with a growth per cycle of approximately 0.1 \AA . As is evident in the SEM images presented in Figure 6, films deposited on SiO_2 and PVD Ta substrates at 130°C are both smooth and uniform. Four point probe sheet resistance measurement of the film on SiO_2 combined with a thickness of 120 \AA yielded a resistivity of $89 \mu\Omega \text{ cm}$.

Film composition was analyzed by XPS depth profiling which revealed that Zn was the main film impurity, with no detectable N and less than 2 at % C detected at all sputter depths. Some interesting trends were apparent in the elemental depth profiling (Figure 7). Most prominently, the outer surface of the film was richer in Zn compared to the bulk of the film where a significantly higher concentration of copper was detected. The binding energies for Cu 2p and Zn 2p on the surface post 30s Ar sputter were 932.6 and 1021.9 eV, respectively, which is consistent with the presence of metallic Cu and Zn and/or their oxides Cu_2O and ZnO , respectively.⁵³ Oxygen was detected at all levels of the depth profile, but the Si/O ratio remains constant after sputtering for 40 s, which suggests that in the bulk of the film, copper and zinc are predominantly in metallic form. The observed electrical conductivity of the film also supports the presence of a substantial amount of metallic Cu and/or Zn in the film, most likely alloyed as a brass. As the depth profile shows, the ratio of Cu/Zn in the film was maximized at approximately 11:1. Attempts to further increase the concentration of Cu in the film by varying the

(52) Barmak, K.; Cabral, C., Jr.; Rodbell, K. P.; Harper, J. M. E. *J. Vac. Sci. Technol., B* **2006**, *24*, 2485.

(53) Hoque, E.; DeRose, J. A.; Houriet, R.; Hoffmann, P.; Mathieu, H. *J. Chem. Mater.* **2007**, *19*, 798.

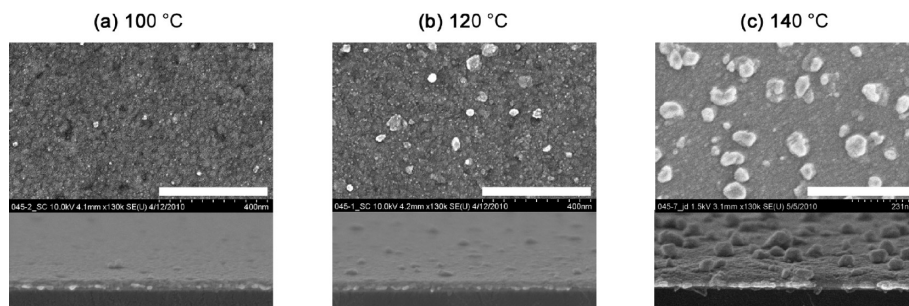


Figure 8. SEM images of CVD films deposited on PVD-Cu using ZnEt_2 at 100–140 °C. Depositions were run using 1000 cycles \times [1 s pulse ZnEt_2 /3 s chamber purge].

substrate temperature between 130 and 150 °C, or the length of purges or precursor/coreactant doses have met with limited success, with Cu:Zn ratios remaining between 6 and 12.

The observed Zn content in the film suggests that reductive decomposition of ZnEt_2 (or its transmetalation products) is occurring as has been suggested for the $\text{ZnEt}_2/\text{H}_2\text{O}$ ALD ZnO process.⁵⁴ Moreover, the increase in Zn concentration close to the surface of the film suggests that this process is self-catalyzed. However, it is also possible that Zn “percolates” to the surface of the film as it grows, leading to a higher Zn concentration near the surface, even if the Cu/Zn ratio for material added in each deposition cycle remains constant. This type of “surfactant” behavior has previously been reported for C in Zn,⁵⁵ I in Cu,⁵⁶ and Bi_2O_3 in LaAlO_3 .⁵⁷

To gain insight into the process of zinc incorporation into the films, CVD of Zn on a copper substrate was attempted at 100, 120, and 140 °C. At 100 and 120 °C, only a small amount of Zn deposition was observed after 1000 \times 1 s pulses, while at 140 °C, CVD of large grains on the surface was observed (Figure 8; zinc deposition was confirmed by XPS). It therefore appears that in ALD/pulsed-CVD experiments using **6b** in combination with ZnEt_2 , zinc incorporation occurs via a parasitic CVD pathway⁵⁸ that becomes far more pronounced at temperatures of 120 °C and above, detracting from the goal of self-limiting deposition (i.e., leading to a pulsed CVD rather than an ALD process). Along similar lines, while Sung and Fischer et al. reported pure copper metal ALD using $[\text{Cu}(\text{OCHMeCH}_2\text{NMe}_2)_2]$ in combination with ZnEt_2 at 100–120 °C, substantial zinc incorporation was observed above 120 °C. Unfortunately, with complex **6b**, similarly low deposition temperatures were not accessible because of a minimum precursor delivery temperature of 120 °C.

Summary and Conclusions

A key factor that has hindered the development of new metal ALD/pulsed-CVD methods is the extremely time-

consuming and resource intensive nature of the process, as well as the requirement for the use of highly specialized equipment. This work demonstrates the usefulness of solution screening methods to identify particularly promising new precursor/co-reagent combinations for metal ALD/pulsed-CVD. On the basis of the solution data, two precursor/co-reagent combinations were selected for more resource and time intensive ALD/pulsed-CVD studies; AlMe_3 and ZnEt_2 with bis(*N*-ethyl-2-pyrrolylaldimine)-copper(II) (**6b**). The co-reagent BEt_3 was also investigated to determine whether lower reactivity (relative to AlMe_3 and ZnEt_2) in solution would translate into reduced ALD/pulsed-CVD reactivity.

As anticipated, no deposition was observed with BEt_3 . However, with AlMe_3 , nonconductive (presumably because of the presence of significant Al_2O_3 impurities after atmospheric exposure) copper-containing films were deposited between 130 and 150 °C. By contrast, with ZnEt_2 , deposition of conductive copper metal films was achieved at 130–150 °C. For films deposited on SiO_2 at 130 °C using a typical pulse sequence, XPS depth profiling revealed that Zn was the main film impurity, with no detectable N and <2 at % C detected at all sputter depths. The maximum copper/zinc ratio was approximately 11:1, with a significant decrease in this ratio near the surface of the film. CVD studies with ZnEt_2 point toward the operation of parasitic ZnEt_2 reduction pathways that become particularly significant at temperatures above 120 °C. Nevertheless, this work highlights the potential of ZnEt_2 and related volatile organometallics as co-reagents for low-temperature late transition metal ALD and pulsed-CVD, and demonstrates the successful implementation of solution screening tests to define the focus of ALD/pulsed-CVD studies.

Mechanistic studies to probe in detail the pathways responsible for the solution deposition of copper films using ZnEt_2 , AlMe_3 , and BEt_3 co-reagents in solution are discussed in a following manuscript.³³ Future studies will focus on strategies to achieve self-limiting deposition and extend these approaches to the ALD/pulsed-CVD of other late transition metals. This work will continue to rely on the high throughput solution screening methodology outlined above, and will target both copper(II) precursors of increased volatility and alternate co-reagents, including new organozinc co-reagents to avoid the reductive decomposition observed with ZnEt_2 .

- (54) Rowlette, P. C.; Allen, C. G.; Bromley, O. B.; Dubetz, A. E.; Wolden, C. A. *Chem. Vap. Deposition* **2009**, *15*, 15 and references therein.
- (55) Cheon, J.; Dubois, L. H.; Girolami, G. S. *Chem. Mater.* **1994**, *6*, 2279.
- (56) Chang, T.-Y.; Tze, J.-J.; Tsai, D.-S. *Appl. Surf. Sci.* **2004**, *236*, 165.
- (57) Molodyk, A. A.; Korsakov, I. E.; Novojilov, M. A.; Graboy, I. E.; Kaul, A. R.; Wahl, G. *Chem. Vap. Deposition* **2000**, *6*, 133.
- (58) Juppo, M.; Ritala, M.; Leskelä, M. *J. Vac. Sci. Technol., A* **1997**, *15*, 2330.

Experimental Section

An argon-filled MBraun UNILab glovebox was employed for the manipulation and storage of all oxygen and moisture sensitive compounds, and air-sensitive preparative reactions were performed on a double manifold high vacuum line using standard techniques.⁵⁹ Residual oxygen and moisture was removed from the argon stream by passage through an Oxisorb-W scrubber from Matheson Gas Products. A Fisher Scientific Ultrasonic FS-30 bath was used to sonicate reaction mixtures where indicated, and a Fischer Scientific Model 228 Centrifuge in combination with airtight Kimble-Kontes 15 mL conical centrifuge tubes was used when required to remove insoluble salts or collect suspended solid for PXRD analysis. Vacuum was measured using a Varian model 531 Thermocouple Gauge Tube with a model 801 Controller. Anhydrous 1,2-dme and diethyl ether were purchased from Aldrich. Hexanes, toluene, and THF were initially dried and distilled at atmospheric pressure from CaH₂, sodium, and sodium benzophenone ketyl, respectively. Unless otherwise noted, all anhydrous protio solvents were stored over an appropriate drying agent prior to use (OEt₂, toluene, C₆H₆ = Na/Ph₂CO; hexanes = Na/Ph₂CO/tetra-lyme). Cu(OMe)₂, Cu(OAc)₂, acetylacetone, 2-pyrrolylaldehyde, salicylaldehyde, isopropylamine, **1**, and **2**·xH₂O were purchased from either Aldrich or Strem Chemicals. Complexes **1** and **2**·xH₂O were obtained from commercial sources, complexes **4**–**7** were prepared as described in the literature,^{16,39,41,42} and complex **3** was prepared from Cu(OMe)₂ and H(acnac)⁶⁰ by a modification of a procedure reported for a related copper(II) β-ketiminate complex.⁶¹ Purple anhydrous **2** was obtained from green **2**·xH₂O by drying under a static vacuum over P₂O₅, followed by sublimation.^{36,37} AlMe₃ (98%), ZnEt₂ (min. 95%), and BEt₃ (98%) were purchased in metal cylinders from Strem Chemicals and stored within an argon-filled glovebox. **NOTE:** AlMe₃, ZnEt₂, and BEt₃ are strongly pyrophoric liquids so must be handled only under strict air-free conditions.

Combustion elemental analyses were performed on a Thermo EA1112 CHNS/O analyzer, and UV–visible spectra were performed using a Varian Cary 50 spectrometer. Thermogravimetric analyses were carried out on 3–10 mg of material sealed inside Al crucibles in a nitrogen atmosphere glovebox. Samples were pierced and exposed to the atmosphere for only a few seconds prior to being placed in a stream of high-purity Ar in the oven of a standard TGA tool and heated at a rate of 10 °C/min. Room temperature magnetic measurements were performed on a Johnson & Matthey magnetic susceptibility balance, and diamagnetic corrections were applied using Pascal's constants.⁶² Single-crystal X-ray crystallographic analyses were performed on crystals coated in Paratone oil and mounted either on: (a) a SMART APEX II diffractometer with a 3 kW Sealed tube Mo generator in the McMaster Analytical X-ray (MAX) Diffraction Facility, Department of Chemistry, McMaster University, Canada, or (b) a Bruker D8 Platform diffractometer with an APEX CCD detector in the Department of Chemistry and

Biochemistry, University of California–San Diego. Powder X-ray Diffraction (PXRD) experiments were performed on a Bruker D8 Advance Powder diffractometer with Cu Kα radiation (λ = 0.154 nm) operated at 40 kV and 40 mA.

[Cu(acnac^{iPr})₂] (**3**) was prepared by a modification of the procedure reported for the *N*-CH₂CH₂OMe analogue.⁶¹ To a solution of H(acnac^{iPr}) (100 mg, 0.709 mmol) in toluene (10 mL) was added copper(II) methoxide (44.5 mg, 0.355 mmol). The mixture was then stirred overnight to give a red-brown solution. After removal of solvent in vacuo, the residue was redissolved in hexanes (5 mL), centrifuged to remove any insoluble impurities, reduced in volume to 2.5 mL, and cooled to –30 °C to yield X-ray quality red-brown crystals of **3** after several days. Yield 95 mg (78%). Anal. Calcd for C₁₆H₂₈N₂O₂Cu: C 55.87, H 8.21, N 8.15. Found: C 56.08, H 8.44, N 8.16%. λ_{max} in toluene = 470 nm (ε = 870 L mol⁻¹ cm⁻¹). μ_{eff}(solid) = 1.91 μ_B at 24 °C.

Solution Deposition Studies. Solution deposition studies were carried out by addition of either 1.0 or 5.0 equiv. of a 150 mM toluene solution of each co-reagent to 1.0 mL of a 15 mM toluene solution of each copper precursor complex in an 8 mL Kimble-Kontes borosilicate screw-cap culture tube with a phenolic screw cap containing a PTFE-faced rubber liner. The resulting 1:1 reactions were 13.6 mM in copper precursor (1.1 mL total solution volume), whereas 1:5 reactions were 10 mM in copper precursor (1.5 mL total solution volume). Using a VWR analog dry block heater, we maintained reactions for 24 h at each of the following temperatures in sequence, 25, 50, 75, 100, 120 °C, and observations were recorded at each of these temperatures. Copper-colored or black powders were analyzed by PXRD and in some cases XPS. Reactions that resulted in the deposition of copper films were repeated in the presence of a Si/SiO₂/Ta/Ru wafer section, and the resulting films were analyzed by SEM and XPS.

Scanning Electron Microscopy (SEM). All samples were sputter-coated with ca. 10 Å of Au/Pd alloy prior to imaging. Imaging was carried out on a standard field-emission electron microscope. Typical working distances were 2.5–4.5 mm. For top down images $V_{acc} = 10$ kV with 15 μA imaging current. For tilt and X-section images $V_{acc} = 5$ kV with 10 μA imaging current.

X-ray Photoelectron Spectroscopy (XPS) of Films Deposited from Solution. X-ray photoelectron spectra were collected on either a Thermo Scientific Thetaprobe or K-Alpha (Thermo Scientific, E. Grinstead, U.K.), both of which are located at the University of Toronto. A monochromated Al K-Alpha was used with a spot size of 400 μm. After an initial survey spectrum was collected on the as-is samples, sputter cleaning was performed to remove the surface oxide and any contamination. The cleaning was followed in a profile mode monitoring Cu, O, C, and Ru intensities. An Ar ion gun was used with 3 kV energy and rastered over either a 2 mm × 2 mm area (K-Alpha) or a 1.5 mm × 1.5 mm area (Thetaprobe). The profile was continued until the C and O values leveled off, or the underlying Ru layer became apparent. The survey spectrum was then obtained at low energy resolution for composition (Cu, O, C, Ru, N, Al, B, and/or Zn), as well as the high-energy resolution spectrum of the Cu 2p_{3/2} region (pass energy 10 eV). Because of the different geometries of the spectrometers, the takeoff angle (relative to the sample surface) was 90 and 55° for the K-Alpha and Thetaprobe, respectively.

X-ray Photoelectron Spectroscopy (XPS) of Films Deposited by ALD/Pulsed-CVD. X-ray photoelectron spectra were collected on a standard XPS tool using a monochromated Al Kα X-ray source and spot size of 400 × 800 μm. Sputtering was performed with a 2 kV Ar⁺ beam rastered over a 4 mm × 4 mm

- (59) Burger, B. J.; Bercaw, J. E., *Vacuum Line Techniques for Handling Air-Sensitive Organometallic Compounds*. In *Experimental Organometallic Chemistry—A Practicum in Synthesis and Characterization*; American Chemical Society: Washington, D.C., 1987; Vol. 357, p 79.
- (60) Tian, X.; Goddard, R.; Pörschke, K.-R. *Organometallics* **2006**, *25*, 5854.
- (61) Baxter, D. V.; Caulton, K. G.; Chiang, W.-C.; Chisholm, M. H.; DiStasi, V. F.; Dutremez, S. G.; Folting, K. *Polyhedron* **2001**, *20*, 2589.
- (62) (a) O'Connor, C. J. *Prog. Inorg. Chem.* **1982**, *29*, 203. (b) Pascal, P. *Ann. Chim. Phys.* **1910**, *19*, 5.

area. The sample was grounded at the surface during depth profiling and no charge neutralization was used. Prior to depth profiling, an initial survey spectrum was collected on the as-received sample. Cu 2p, Zn 2p, Si 2p, C 1s, O 1s, and N 1s spectra were acquired during the profile. Post-sputter, the C 1s signals were located in the baseline indicating less than 2 at % C at all sputter depths and could not be accurately integrated.

X-ray Photoelectron Spectroscopy (XPS) of ZnEt₂ Pulsed CVD Films on PVD Ta/Cu Substrates. X-ray photoelectron spectra were collected on a Thermo Scientific ESCALAB 250 instrument (ThermoScientific, East Grinstead, UK) at the CAMCOR Surface Analytical Facility, University of Oregon. A monochromated Al K α X-ray source was used with a spot size of 250 μ m. Sputtering was performed with a 1 kV Ar⁺ beam rastered over a 2 mm \times 2 mm area. Surfaces were analyzed as received as well as post 15s Ar⁺ sputter. Cu 2p, Zn 2p, Si 2p, C 1s, O 1s, and N1s spectra were acquired. The takeoff angle (relative to the sample surface) was 90 $^\circ$.

Substrates for ALD/Pulsed-CVD or CVD Experiments. Substrates were prepared as follows: (i) SiO₂; 1 k \AA thermally grown SiO₂/Si films were used as received; (ii) PVD Ta & PVD Ta/Ru; 1 k \AA thermally grown SiO₂/Si substrates received a standard RCA clean prior to the physical sputter of 150 \AA Ta or 150 \AA Ta plus 370 \AA Ru metal without an air-break, respectively; (iii) PVD Ta/Cu; 1k \AA SiO₂/Si substrates received a standard RCA clean prior to the physical sputter of 100 \AA Ta followed by 300 \AA Cu without air break. All substrates were exposed to the atmosphere prior to ALD/pulsed-CVD or CVD.

Atomic Layer Deposition/Pulsed-CVD. ALD/pulsed-CVD experiments were carried out in a standard horizontal, hot wall traveling wave ALD reactor. The chamber received a 2 h, 250 $^\circ$ C nitrogen purge with pulsed forming gas prior to starting ALD/

pulsed-CVD deposition. The typical deposition pressure was 30 Pa (0.3 Torr) with 1 slm. N₂ (99.999%) carrier gas. Diethylzinc (Crompton GmbH), trimethylaluminum (Crompton GmbH), and triethylborane (Sigma-Aldrich, Inc.) were used as received and were held at room temperature during delivery. The Cu precursor **6b** was held in a solid source vaporizer at 120 $^\circ$ C. A schematic of the ALD reactor can be found in the ESI. Typical ALD/pulsed-CVD runs done at 130 $^\circ$ C – 150 $^\circ$ C substrate temperatures with different coreactants were as follows: ZnEt₂, 1500 \times [6 s ZnEt₂/7 s purge/3 s **6b**/7 s purge]; AlMe₃, 1000 \times [3 s **6b**/7 s purge/0.3 s AlMe₃/7 s purge]; BEt₃, 5000 \times [0.4 s BEt₃/1.8 s purge/1.5 s **6b**/1.8 s purge]. Samples were cooled to <60 $^\circ$ C prior to removal from the reactor.

CVD Using ZnEt₂. CVD studies were carried out on PVD Ta/Cu substrates. Substrates were heated to 150 $^\circ$ C in the same ALD chamber used for the atomic layer deposition/pulsed CVD experiments. Forming gas was flowed through chamber for 500 s. The chamber temperature was then stabilized at the desired substrate temperature prior to 1000 cycles of 1 s ZnEt₂/3 s purge.

Acknowledgment. D.J.H.E. is grateful for funding provided by Intel Corporation and the Emerging Materials Knowledge (EMK) program of Ontario Centres of Excellence (OCE), Canada. We thank Dr. Rana Sodhi of Surface Interface Ontario, University of Toronto, Canada, and Dr. Stephen Golledge, CAMCOR, University of Oregon, for acquisition of XPS data.

Supporting Information Available: Additional surface characterization and experimental details (PDF); X-ray crystallographic data (CIF). This material is available free of charge via the Internet at <http://pubs.acs.org>.